Proceeding of the 2004 American Control Conference
Boston, Massachusetts June 30 - July 2, 2004

Experimental Verification of the Dynamic Model for a Quarter Size Self-Balancing Wheelchair

Adam Blankespoor
Department of Mechanical Engineering
University of Utah
Salt Lake City, UT 84102, USA
a.blankespoor@utah.edu

Robert Roemer
Department of Mechanical Engineering
University of Utah
Salt Lake City, UT 84102, USA
bob.roemer@utah.edu

***Abstract*— A quarter size scale model of the Sitting-Standing Transporter (SST), a self-balancing wheelchair capable of supporting a person in the sitting and standing position, was designed, constructed, and tested. The scale model represents a loaded wheelchair with only two parallel wheels. The chair and a counter balance are both attached to the main axle and are free to rotate around it. In order to keep the chair in a stable position above the main axle, a state-feedback controller is used to drive the wheels and control the position of the counter balance. The controller used to stabilize the scale model in this research was a Linear Quadratic Regulator (LQR) with five inputs and two outputs. The performance of the scale model was evaluated with five tests that represent situations that would be encountered in everyday use of the SST. These tests were also simulated using a nonlinear dynamic model and these simulation results were compared to the experimental results. Based on the comparison between simulation and experimental results, the accuracy of the dynamic model was verified. The dynamic model and the scale model can now be used to provide insights into building a full size SST.**

I. INTRODUCTION

Most people hardly think twice about going up a flight of steps or walking on a sidewalk in a busy city. On the other hand, for approximately one and a half million people, independent mobility is a significant problem [1]. Daily, these individuals must face limitations of access due to curbs, steps, and irregular terrain that a wheelchair cannot easily overcome. In addition to limitations on mobility, there are also adverse physical and psychological consequences of using a standard wheelchair and being confined to the subordinate sitting position [2-5]. A paradigm shift in wheelchair design is needed in order to develop a holistic solution for wheelchair users. An improved design would increase mobility and reduce physical and psychological problems caused by using a standard wheelchair.

A group of self-balancing wheelchairs has shown promise in providing wheelchair users increased mobility. The increased mobility is accomplished by removing the small castor wheels needed for stability. Instead, these wheelchairs balance on the larger rear wheels, which have a greater ability to roll over obstacles. Three alternative designs for maintaining balance have surfaced over the years, the simple inverted pendulum [6-9], the double inverted pendulum [10], and the inverted pendulum with counter balance [11,12]. The simple inverted pendulum is a wheelchair with two parallel wheels and a chair supported above the main axle. The double inverted pendulum also has two parallel wheels, but locates the drive motors and batteries above the main axle and the chair above the motor and battery unit. The inverted pendulum with counter balance places the chair above the axle connecting the wheels and the motors and batteries are housed in a counter balance that swings below the main axle under the control of a third motor.

All three of these self-balancing designs have merit, but a comparative analysis using simulations has shown that the inverted pendulum with counter balance is the superior mechanical design. Another researcher used computer simulations to perform comparative testing on the three designs [12]. He simulated each design type in a number of situations and scored each design based on its overall performance. Using criteria such as minimum preactuation, accelerations on the user, power consumption, and overall stability, he concluded that the inverted pendulum with counter balance was the best mechanical configuration for a self-balancing wheelchair.

The sitting-standing transporter (SST) design is based on the inverted pendulum with counter balance. It will retain the size and basic form of a standard wheelchair, with two large drive wheels in the rear and two castors in the front. However, in addition to operating in the standard manner, this automatic wheelchair will also balance on its back wheels. In order to achieve physical and psychological benefits of standing [2,4,5,13], the SST will also support the user in the standing position in both the two and four wheel modes of operation.

In this paper, a quarter size scale model of the SST will be presented. The scale model has served as a means to experimentally verify the dynamic model used to design the linear quadratic regulator (LQR), which stabilized the inverted pendulum. This verified dynamic model can then be used for further controller design and testing. The scale model, which produces reasonable results, can also be used for testing situations that would be difficult to simulate due to system nonlinearities and other ”real world” complications.

0-7803-8335-4/04/$17.00 ©2004 AACC

TABLE I

SCALING PARAMETERS [12]

Parameter	Scaling Factor
Length	1/4
Mass	1/64
Inertia	1/1024
Torque	1/256
Time	2/1
Position	1/1
Velocity	2/1
Acceleration	4/1

II. QUARTER-SIZE SCALE MODEL

In order to assure similar results between the full size SST and the scale model, a dimensional analysis was performed to find the scaling parameters that would ensure accurate comparisons between the full size and scale model. (Table 1 shows the scaling parameters.) The SST was modeled in two dimensions with the following equations of motion:

$$T_{cb} = m_c r_c^2 \ddot{\theta}_c + I_c \ddot{\theta}_c + m_c \ddot{\theta}_w r_w r_c cos(\theta_c) - m_c g r_c sin(\theta_c) \quad (1)$$

$$T_{cb} + T_w = m_c r_w r_c \dot{\theta}_c^2 sin(\theta_c) + m_c r_w r_c \ddot{\theta}_c cos(\theta_c) - m_c r_w^2 \ddot{\theta}_w - m_c r_w^2 \ddot{\theta}_w - I_w \ddot{\theta}_w - m_{cb} r_{cb} r_w \dot{\theta}_c^2 sin(\theta_c) + m_{cb} r_{cb} r_w \ddot{\theta}_{cb} cos(\theta_{cb}) - m_w r_w^2 \ddot{\theta}_w \quad (2)$$

$$T_w = -m_{cb} r_{cb} r_w \ddot{\theta}_w cos(\theta_{cb}) + m_{cb} r_{cb}^2 \ddot{\theta}_{cb} + I_{cb} \ddot{\theta}_{cb} + m_{cb} g r_{cb} sin(\theta) \quad (3)$$

T - represents the motor torque
m - represents the mass
r - represents the length to the center of mass
I - represents the rotational inertia
c - describes variables for the chair
cb - describes variables for the counter balance
w - describes variables for the wheels
θ - describes the angles (states)

The equations 1 through 3 are the three equations for the three degrees of freedom, the angle of the chair, the angle of the counter balance, and the angle of the wheels, respectively.

In order to design the LQR controller, this model was linearized by setting cos(θ) = 1, sin(θ) = θ, and (dθ/dt)^2 = 0 for each system angle, and converted to the state space form,

$$\dot{x} = Ax + Bu \quad (4)$$

In the linearized model, *A* and *B* are the coefficient matrices for the states (*x*) and inputs (*u*), respectively. The gain matrices *Q* and *R* where determined by the necessary gains to reduce the angular displacement and its derivatives of the chair and therefore the user. The five states are defined by the angles and angular velocities shown in Fig. 1. The inputs are the wheel motor torque and counter balance motor torques, also shown in Fig. 1, and are based on the state vector, accomplishing state feedback by the following:

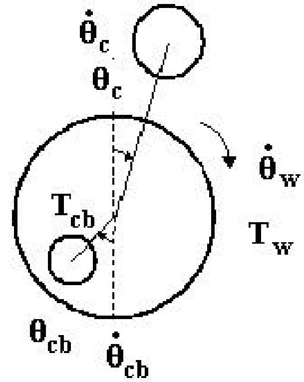

Fig. 1. State (x) and Input (u) definitions

$$u = -Kx \quad (5)$$

where K is the gain matrix found by solving the Riccati equation [14].

The five states are measured with three sensors; a gyroscope, a potentiometer, and a tachometer. The gyroscope measures the angular velocity of the chair, and this value is integrated to find the angle of the chair. The potentiometer is mounted to the counter balance and measures the relative displacement between the counter balance and the chair. Using the chair angle from the gyroscope, the absolute angle of the counter balance is determined. This absolute angle is also differentiated in order to find the angular velocity of the counter balance. Finally, the tachometer is mounted to the counter balance and measures the relative angular velocity of the wheel. Using the known angular velocities from the previous two sensors, the absolute velocity of the wheels is determined.

A SIMULINK[1] program was used, with the nonlinear model of the plant, to design and test the controller in simulation. Simulations with a variety of initial conditions and disturbances were conducted, which were compared to the experimental results in order to verify the simplified linear model used to design the controller. The LQR controller was implemented on a dSPACE[2] system, which uses SIMULINK programs to compile the controller code to a PowerPC which runs the controller real time. Fig. 2 shows a schematic of the experimental setup, including the scale model, computer, motors, and amplifiers.

III. EXPERIMENTAL RESULTS

Five different tests were conducted on the physical scale model. Each test was compared to the results found in simulation. Fig. 3 shows the SST balancing under the guidance of the controller. While balancing, the wheels would roll

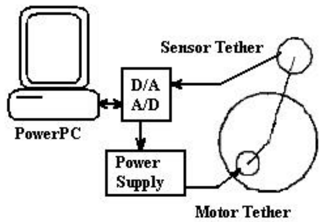

Fig. 2. Experimental setup

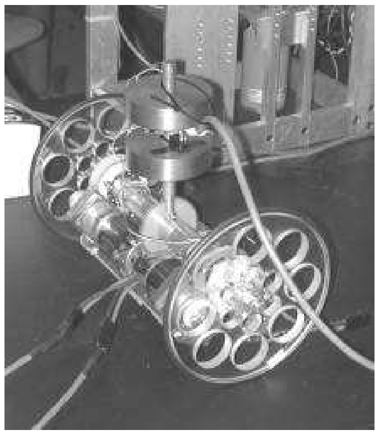

Fig. 3. Scale model of the SST balancing

back and forth to maintain balance. The largest angular displacement was 0.14-radians, or 1.07-cm. of translational motion

1) Disturbance Rejection: This test measured the SST's ability to reject disturbances. It was conducted by giving the model a reference input of zero (all states set to zero) while tapping the chair by hand. A similar disturbance test was also simulated. Unfortunately, tapping the SST by hand was difficult to quantify, so a direct comparison between experiment and simulation was not possible. Thus, to provide comparable results, the disturbance value in the simulations was decreased until the maximum simulation output angles were similar to the maximum experimental angles. Simulation results with a maximum impact force of 0.5 N over 0.5 seconds at the top of the chair are presented. The impact caused an experimental angular displacement of the wheels equal to 1.25-radians, or 9.52-cm. Experimental and simulation results can be seen in Fig. 4

2) Initial Angle Offset: This test measured the ability of the controller to stabilize the system when the initial states were not all zero by setting the initial chair angle at nonzero values, releasing the chair, and seeing if the chair could recover from the initial offset. The largest initial angle that the controller could compensate for was found to be 16.4 degrees. Fig. 5 shows the results from an initial offset of 14.6 degrees. As expected, the wheels were turned to move the main axle beneath the chair's center of gravity in order to maintain balance. The resulting overall translation of the SST was 1.9 centimeters. Fig. 5 also shows

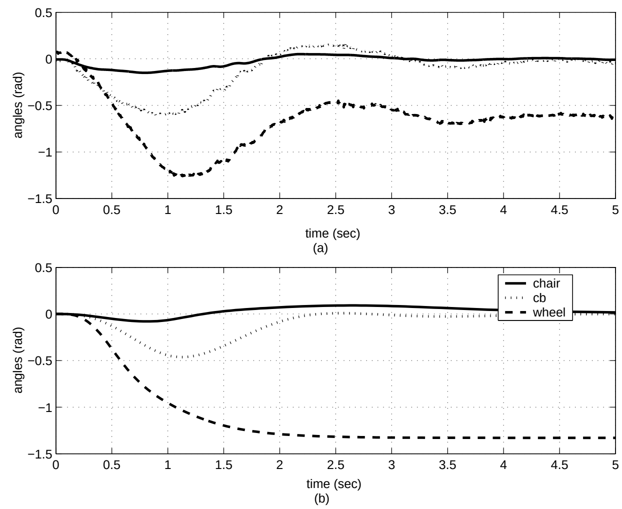

Fig. 4. Disturbance rejection test results for (a) experiment and (b) simulation

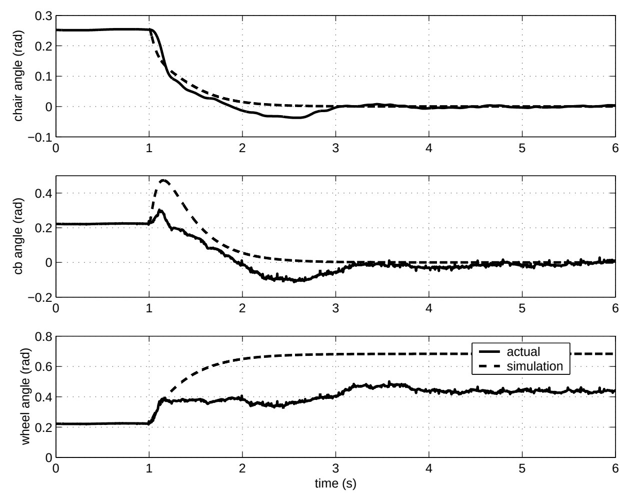

Fig. 5. Experimental and simulation results showing the three output angles for initial angle offset

a direct comparison between the experimental results and the simulation results.

3) Physical Parameter Sensitivity: Without changing the mathematical model or the controller gains, extra mass was added to the top of the chair to investigate the system's sensitivity to changes in the physical system. A 90-gram disk was placed on the top of the chair, which increased the chair's rotational inertia by 17 percent and the height of its center of gravity by 5 percent. With the added mass, the disturbance rejection test was repeated. Fig. 6 shows the experimental wheel angles (a) and the simulation wheel angles (b) for both the modelled mass and the extra mass cases.

4) Controller Gain Sensitivity: The sensitivity of the system to the controller gains was tested by changing the gains of the controller and repeating the initial angle offset test. The ten gains were increased from 1.01 times to 1.25

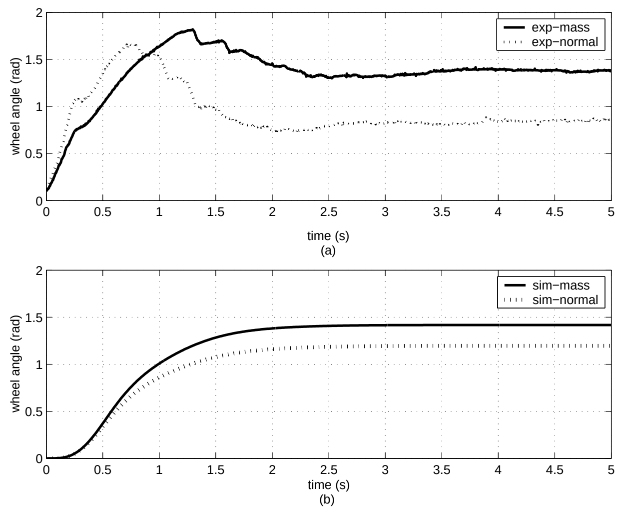

Fig. 6. Test results for (a) experimental and (b) simulation comparisons of disturbance rejection for standard case and extra mass case.

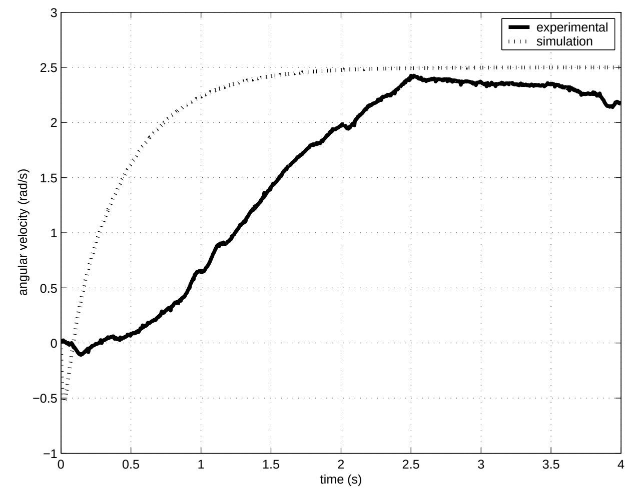

Fig. 8. Experimental and simulation results for velocity step input

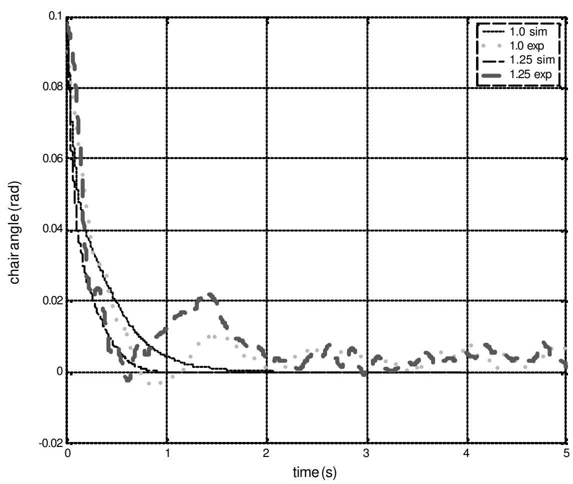

Fig. 7. Experimental and simulation results for the controller gain sensitivity test

times the nominal value in separate tests. Each test was conducted with the same initial offset of 0.1 radians (5.7 degrees). The results for all of the tests were very consistent, so only one data set is shown. Fig. 7 shows the nominal gain and 1.25 times the nominal gain in experiment and simulation.

5) Velocity Step Input Test: A step input of 2.5 rad/s for the wheel angular velocity was given as the reference input to the controller. The experimental angular velocity of the wheel can be seen in Fig. 8 compared to the simulation result. The simulation had a rise time of 1.7 seconds, while the scale model had a rise time of 2.4 seconds.

IV. Discussion

Five experiments were performed and compared to simulations. The comparisons were done in an attempt to verify the dynamic model used to design the controller so further research could be conducted on the SST. As shown in Fig. 3 through Fig. 8, the scale model controller was able to stabilize an inherently unstable system and perform well with a variety of disturbances, initial conditions, and plant-model mismatch. All of the experimental results were qualitatively the same as the simulation results.

Several quantitative differences were observed. One difference observed was the overshoot measured in the disturbance tests (Fig. 4 and Fig. 6). Both of the experiment wheel angular displacements displayed more overshoot than found in simulations. As stated in the previous section, tapping the SST by hand was difficult to simulate exactly. No time was spent developing an exact measurement of the force value and impact duration for use in simulation. Therefore the difference between the experiment and simulation can be explained by a deficiency in the disturbance modeling and not the dynamic model or nonlinearities in the hardware, e.g. the tether.

Another difference occurs in the velocity step input test (Fig. 8). The experimental wheel speed was a little slower than 2.5 rad/s, and the settling time was also a little longer (2.4 seconds, compared to 1.7 seconds). This difference could be due to the tether. The tether contributed an unmodeled contribution to the SST's dynamics, and could add a dampening effect to the system to explain the slower response time.

Overall, the comparisons between the experimental results and the simulation results were very close. The agreement between simulation and experimental results indicates a reliable dynamic model and scaling process. The simplifications and assumptions used to develop the dynamic model retain enough detail to accurately predict the SST's performance. With the dynamic model verified, simulations can be used with confidence for further controller development. The physical SST can also be used for further experimental testing when simulation results are not available or difficult to obtain.

Finally, the design and construction of the full size SST could be carried out in a similar fashion of that used for the quarter size model. The mathematical model used to design the controller does not need any major revisions. The basic design of the main axle assembly, where the wheels, counter balance, and chair meet could also be used for the full size design. One desirable goal would be to eliminate the tether, and implement the power and control systems on the SST. More care will be necessary in the implementation of safety considerations in the full size design, since people will be riding in the chair. If turning was desired, more time would need to be invested in model development and testing.

V. CONCLUSION

The goal of this research was to design, build, and test a quarter size scale model of the SST. The motivations for the quarter size model were to verify the dynamic model used to design the controller and develop a useful tool for building a full size SST.

In the previous sections, the results of the tests were reported and analyzed. The experimental results were compared to the results obtained in simulations. All of the experimental results were qualitatively similar to the simulations. The main differences were in response times and percent overshoot. The model of the SST used to design the controller neglected many of the nonlinearities of the system including the influence of the tether. Therefore, some differences between experiment and simulation would be expected. On the other hand, based on the similarity between the experimental and simulation results in a number of tests, and the simple fact that the controller is able to stabilize an unstable system, the dynamic model of the SST provides a realistic representation of the system.

In summary, the dynamic model of the SST has been experimentally verified. Two tools, the dynamic model and the physical scale model, are now available for further development of the SST.

REFERENCES

[1] Russel, J. N., Hendershot, G. E., Leclere, F., Howie, L. J., and Adler, M., Trends and differential use of assistive technology devices: United States, *Advance data from vital and health statistics*, no. 292, 1994, National Center for Health Statistics, Hyattsville, Maryland.

[2] Bromley, I., Tetraplegia and Paraplegia, *A Guide for Physiotherapists, 5th ed.*, Churchill Livingstone, New York; 1998.

[3] DeLisa, J. A., Ed., Rehabilitation Medicine, *Principles and Practice, 3rd ed.*, Lippincott-Raven, Philadelphia; 1998.

[4] Kaplan, P. E., Roden, W., Gilbert, E., Richards, L., and Goldschmidt, J. W., Reduction of hypercalciuria in tetraplegia after weight-bearing and strengthening exercises, *Paraplegia*, Vol. 19, No. 5, 1981, pp. 289-293.

[5] Gould, D. W., Hsieh, A. C. L., and Tinckler, L. F., The effect of posture on bladder pressure, *Journal of Physiology*, Vol. 129, 1955, pp. 448-453.

[6] Walker, S. D., Roemer, R. B., and Dennison, J., Self-balancing two-wheeled wheelchair: State space control feasibility and prototype test results, *Proceedings, ASME Winter Annual Meeting: Advances in Bioengineering*, 1983, pp. 86-87.

[7] Takahashi, Y. Takagaki, T. Kishi, J. and Ishii, Y., Back and forward moving scheme of front wheel raising for inverse pendulum control wheelchair robot, *Proceedings of the 2001 IEEE International Conference on Robotics and Automation*, Seoul Korea., May 21-26, 2001, pp. 3189-3194.

[8] Yamafuji, K., Hirabayashi, T., Naruse, T., Postural and driving control of the controlling arm-wheel-type parallel bicycle, *Proceedings of the 20th International Symposium on the Industrial Robotics*, 1989, pp. 227-234.

[9] Kamen, D., Ambrogi, R., Duggan, R., Heinzmann, R., Key, B., Dastous, S., Control loop for transportation vehicles, *United States Patent*, No. 5791425, 1998.

[10] Jorgensen, G. H. and Garbini, J. L., Dynamic analysis and control of traversing stairs with an actively stabilized wheelchair, *Proceedings, 1997, 1st IEEE/ASME International Conference on Advanced Intelligent Mechatronics*, Tokyo, Japan, 1997, pp. 118.

[11] Dennison, J., Ashqar, M., Costa, V., Johnson, M., and Malhiot, K., Self- Balancing Wheelchair, *Senior Design Report, Mechanical Engineering*, UC Santa Barbara, Santa Barbara, 1979.

[12] Olson, Z. L., A comparative analysis of three self-balancing wheelchair balancing mechanisms, *Master of Science, Mechanical Engineering*, University of Utah, Salt Lake City, 2001.

[13] Cahill, S. and Eggleston, R., Reconsidering the stigma of physical disability: Wheelchair use and public kindness, *Sociological Quaterly*, Vol. 36, No. 4, 1995, pp. 681-699.

[14] Friedland, B., *Control System Design: An Introduction to State-Space Methods*, McGraw Hill, New York; 1986.